

## ARTICLE

# Sorbitol Hydrogenolysis to Glycols over Basic Additive Promoted Ni-based Catalysts

Xiao-feng Cao<sup>a,c</sup>, Qi Zhang<sup>b</sup>, Dong Jiang<sup>a\*</sup>, Qi-ying Liu<sup>b\*</sup>, Long-long Ma<sup>b</sup>, Tie-jun Wang<sup>b</sup>, De-bao Li<sup>a</sup>

a. State Key Laboratory of Coal Conversion, Institute of Coal Chemistry, Chinese Academy of Sciences, Taiyuan 030001, China

b. CAS Key Laboratory of Renewable Energy, Guangzhou Institute of Energy Conversion, Chinese Academy of Sciences, Guangzhou 510640, China

c. University of Chinese Academy of Sciences, Beijing 100049, China

(Dated: Received on January 19, 2015; Accepted on April 9, 2015)

A series of Ni based catalysts with different supports and basic additives were prepared by sequential impregnation method. The catalysts were characterized by XRD, BET, H<sub>2</sub>-TPR and CO<sub>2</sub>-TPD techniques. It was found that the introduction of basic additives enhanced the basicities of catalysts and promoted the dispersities of Ni particles by strong interaction between Ni<sup>2+</sup> and basic additives. Among the Ni based catalysts, 10%Ni/10%La<sub>2</sub>O<sub>3</sub>/ZrO<sub>2</sub> showed the superior performance in sorbitol hydrogenolysis. The synergistic effect of Ni and La<sub>2</sub>O<sub>3</sub> was proven to play an essential role in selective synthesis of EG and 1,2-PG. In the optimal reaction condition, the catalyst presented 100% sorbitol conversion and over 48% glycols (EG and 1,2-PG) yield. The kinetics study of polyols (sorbitol, xylitol and glycerol) hydrogenolysis showed that polyols with more hydroxyl number have higher activity and products distribution was final results of kinetic balance, which could give us some inspiration about how to change the products selectivity.

**Key words:** Sorbitol hydrogenolysis, Glycols, Ni catalyst, Support, Base promoter

## I. INTRODUCTION

Efficient transformation of biomass to valuable chemicals has received increasing concerns during the past decades because of its abundant, renewable, wide distribution and carbon neutral properties when compared to the traditional fossil resources [1, 2]. Sorbitol is an important biomass-derived platform compound [3, 4] and diversified downstream chemicals can be obtained by hydrogenolysis, dehydration, hydrodeoxygenation, oxidation processings. Sorbitol hydrogenolysis is an interesting way to produce polyols such as glycerol, ethylene glycol (EG), and propylene glycol (1,2-PG). These products are widely used to manufacture polyesters resins, surfactants, and pharmaceuticals [5, 6].

According to the polyols hydrogenolysis mechanism [7, 8], sorbitol hydrogenolysis generally undergoes complex reaction pathways to the final products and byproducts including dehydrogenation over metal sites of catalyst and retro-aldol condensation of the intermediates to produce C2 or C3 polyols over basic sites of support and/or basic additive. Thus sorbitol hydrogenolysis needs the synergistic effect of metal and

base sites to promote the reaction. Currently, conventional hydrogenation catalysts such as Ni, Cu, Ru, and Pt [9–17] based catalysts were mainly used for the sorbitol hydrogenolysis. For example, Zhao *et al.* prepared Ru/CNFs by incipient wetness impregnation for sorbitol hydrogenolysis and the higher activity and selectivity for glycols were obtained compared with Ru supported on commercial activated carbon [14, 16]. Banu *et al.* reported that 1,2-propanediol was the major product in sorbitol hydrogenolysis using Ni/NaY as the catalyst, however, when Ni was replaced by Pt, glycerol was presented as the main product in the same process [9, 17]. These results showed that besides metal, the effect of support and basic additive was significant in activity and product distribution [9, 11, 17–22], but the relative investigation was rarely reported.

In this work, we prepared diversified Ni based catalysts with different support and basic additive by sequential impregnation method. The physicochemical properties of the catalysts were characterized by N<sub>2</sub> adsorption-desorption isothermal curves, powder X-ray diffraction (XRD), H<sub>2</sub>-temperature programmed reduction (H<sub>2</sub>-TPR), CO<sub>2</sub>-temperature programmed desorption (CO<sub>2</sub>-TPD) techniques. The catalytic performances of catalysts were tested in sorbitol hydrogenolysis to glycols and the influence of support and basic additive was elucidated. We also studied the kinetic process of polyols hydrogenolysis to investigate the in-

\* Authors to whom correspondence should be addressed. E-mail: jdred@sxicc.ac.cn, liuqy@ms.giec.ac.cn, Tel.: +86-351-4041209/+86-20-87048614, FAX: +86-351-4041153/+86-20-87057789

fluence of the products selectivity of sorbitol hydrogenolysis.

## II. EXPERIMENTS

### A. Catalyst preparation

The supports  $ZrO_2$ ,  $ZnO$ ,  $\gamma-Al_2O_3$ , and  $SiO_2$ ,  $Ni(NO_3)_2 \cdot 6H_2O$ ,  $La(NO_3)_3 \cdot 6H_2O$ ,  $Mg(NO_3)_2 \cdot 6H_2O$ ,  $(NH_4)_2Ce(NO_3)_6$ , and  $Ca(NO_3)_2 \cdot 4H_2O$  were obtained commercially and used as received.

Ni based catalysts were prepared by sequentially initial wetness impregnation. With  $Ni/La_2O_3/ZrO_2$  catalyst as an example, a certain amount of  $La(NO_3)_3 \cdot 6H_2O$  was dissolved in deionized water, followed by introducing  $ZrO_2$ . This mixture was aged for 3 h under agitation and then evaporated excessive  $H_2O$  at  $80^\circ C$  to obtain white powder. The solid was further dried overnight at  $100^\circ C$  and then calcined at  $550^\circ C$  for 4 h to obtain  $La_2O_3/ZrO_2$ . For the second impregnation,  $Ni(NO_3)_2 \cdot 6H_2O$  was dissolved in deionized water and the impregnation procedure was similar to  $La_2O_3/ZrO_2$ . After drying at  $100^\circ C$ , the  $Ni/La_2O_3/ZrO_2$  was calcined at  $550^\circ C$  in static air for 4 h. Similarly the Ni based catalysts with different support and basic additive were prepared with 10% of Ni loading and 10% of basic additives. Before reaction, the catalyst was reduced in  $H_2$  at  $500^\circ C$  for 4 h (for  $Al_2O_3$ -supported catalyst, the reduction was implemented at  $750^\circ C$  for 4 h).

### B. Catalyst characterization

$N_2$  adsorption-desorption isothermal curves were obtained at  $-196^\circ C$  on a Micromeritics ASAP 2420 instrument. Prior to the measurement, the samples were degassed under vacuum for 8 h at  $250^\circ C$ .

XRD patterns of the catalysts were obtained by using X'pert PRO MPD diffractometer (PANalytical) with a  $Cu K\alpha$  ( $\lambda=0.15406$  nm) radiation operated at 40 kV and 40 mA.

$CO_2$ -TPD and  $H_2$ -TPR curves were carried out in Automatic chemical adsorption instrument from Quantachrome. In a typical run, about 50 mg reduced sample was loaded in a U-shaped quartz tube. Prior to the measurement, the catalyst sample was pretreated in He at  $250^\circ C$  for 1 h, then cooled to  $50^\circ C$  and was saturated with pure  $CO_2$  for 1 h. After being purged with He for 40 min to remove the physically adsorbed  $CO_2$ , the sample was heated from  $50^\circ C$  to  $850^\circ C$  at  $10^\circ C/min$  and the  $CO_2$  desorption was monitored with a TCD detector.

$H_2$ -TPR curves were obtained through similar procedure. In a typical run, about 20 mg sample was loaded in a U-shaped quartz tube. Prior to the measurement, the catalyst sample was pretreated in He at  $250^\circ C$

for 1 h, then cooled to  $50^\circ C$ . The sample was heated from  $50^\circ C$  to  $850^\circ C$  at  $10^\circ C/min$  in a 60 mL/min of 5% $H_2/N_2$  flow. The  $H_2$  sorption was monitored with a TCD detector.

### C. Sorbitol hydrogenolysis and products analysis

Sorbitol hydrogenolysis was carried out in a 100 mL stainless steel autoclave with agitation. After 20 mL of 100 mg/mL sorbitol aqueous solution and 0.4 g catalyst were introduced, the reactor was purged with  $H_2$  for five times to remove the residual air, aerated to the initial 4 MPa of  $H_2$  pressure and then heated to a desired reaction temperature under rigorous stirring. After certain duration, the autoclave was cooled down rapidly in cold water.

The aqueous products were analyzed by HPLC (Waters e2695) equipped with a differential refraction detector (RID 2414). The separation of products was achieved using an Aminex HPX-87H column at  $45^\circ C$ . Aqueous solution of sulphuric acid (0.005 mol/L  $H_2SO_4$ ) was used as the mobile phase at a flow rate of 0.55 mL/min. Sorbitol conversion and products selectivity were calculated based on the carbon balance using a typical external standard procedure.

The conversion  $X$  of sorbitol and selectivity  $S(i)$  of product  $i$  were defined as:

$$X = \frac{\rho_0 - \rho_1}{\rho_0} \times 100\% \quad (1)$$

$$S(i) = \frac{n_i M_0}{6(\rho_0 - \rho_1)} \times 100\% \quad (2)$$

here  $\rho_0$  refers to the initial concentration of sorbitol,  $\rho_1$  means the final concentration of sorbitol after reaction,  $n_i$  refers to molar amount of the product  $i$  (glycerol, EG, and 1,2-PG), and  $M_0$  is molar mass of sorbitol.

## III. RESULTS AND DISCUSSION

### A. Chemical and physical properties of catalysts

Table I summarized the textural properties of Ni supported on  $ZrO_2$ ,  $ZnO$ ,  $\gamma-Al_2O_3$ , and  $SiO_2$  with and without  $La_2O_3$  as the additive. Compared to the pristine support, Ni impregnation resulted in reduction of surface area for all investigated supports together with the slightly increased average pore diameters. However, no obvious tendency was observed for the pore volumes. When  $La_2O_3$  was introduced, followed by impregnating Ni, the surface area, pore volume and size of the catalysts almost kept unchanged except for the support  $\gamma-Al_2O_3$ . We also calculated the consistency size of supported NiO by using the (111) facet and Scherrer equation. Compared to the Ni catalysts without  $La_2O_3$ , the addition of  $La_2O_3$  significantly reduced the NiO crystal size no matter what kinds of supported was employed,

TABLE I The textural properties and NiO size of La<sub>2</sub>O<sub>3</sub> promoted Ni catalysts on difference supports.

Sample	$S_{\text{BET}}^{\text{a}}/(\text{m}^2/\text{g})$	Pore volume/ $(\text{cm}^3/\text{g})$	Average pore diameter/nm	NiO grain size <sup>b</sup> /nm
ZrO <sub>2</sub>	40.3	0.17	16.5	
10%Ni/ZrO <sub>2</sub>	35.0	0.18	21.1	50
10%Ni/10%La <sub>2</sub> O <sub>3</sub> /ZrO <sub>2</sub>	35.7	0.16	18.1	15
ZnO	10.3	0.034	13.1	
10%Ni/ZnO	5.2	0.044	34.1	50
10%Ni/10%La <sub>2</sub> O <sub>3</sub> /ZnO	6.4	0.053	33.1	25
$\gamma$ -Al <sub>2</sub> O <sub>3</sub>	135.8	0.60	17.8	
10%Ni/ $\gamma$ -Al <sub>2</sub> O <sub>3</sub>	115.4	0.57	19.7	31
10%Ni/10%La <sub>2</sub> O <sub>3</sub> / $\gamma$ -Al <sub>2</sub> O <sub>3</sub>	95.5	0.43	17.8	25
SiO <sub>2</sub>	145.1	0.93	25.7	
10%Ni/SiO <sub>2</sub>	122.6	0.79	25.9	28
10%Ni/10%La <sub>2</sub> O <sub>3</sub> /SiO <sub>2</sub>	122.6	0.82	26.8	10

<sup>a</sup> BET surface area was measured by N<sub>2</sub>-adsorption-desorption isothermal curve.

<sup>b</sup> NiO crystal size was calculated, depending on the crystallographic (111) plane by Scherrer equation.

which indicated that La<sub>2</sub>O<sub>3</sub> can improve the dispersity of Ni on catalyst.

XRD patterns of Ni based catalysts are presented in Fig.1. The diffractions of NiO were found when it was loaded on different supports without La<sub>2</sub>O<sub>3</sub>. The diffraction peaks at 37.3°, 43.3°, and 62.9° for 2 $\theta$  were attributed to the (111), (200), and (220) crystal planes of NiO. The diffraction peaks corresponding to NiO became weaker when La<sub>2</sub>O<sub>3</sub> was introduced on the supports, which indicated La<sub>2</sub>O<sub>3</sub> improved the dispersity of NiO by the enhanced interaction between Ni<sup>2+</sup> and La<sub>2</sub>O<sub>3</sub> [18]. Besides La<sub>2</sub>O<sub>3</sub>, the enhanced dispersities for NiO were also observed when using CeO<sub>2</sub>, MgO and CaO as the promoters and ZrO<sub>2</sub> as the support (Fig.S1 in supplementary material). Here, the diffractions of La<sub>2</sub>O<sub>3</sub> and other basic promoters were not detected in the Ni based catalysts, indicating the high dispersity of these additives resulted from their amorphous properties or very tiny particles below the XRD detection threshold [19]. The reduced NiO particle sizes are very consistent with those obtained by the calculation of Scherrer equation (Table I).

The basicities of Ni based catalyst with different supports and La<sub>2</sub>O<sub>3</sub> are shown in Fig.2. As Ni was supported on ZrO<sub>2</sub>,  $\gamma$ -Al<sub>2</sub>O<sub>3</sub> and SiO<sub>2</sub>, the CO<sub>2</sub> desorption peaks centered at about 150 °C and the shoulders at about 300 °C were observed, indicating weak and medium basicities were simultaneously presented on the surface of Ni based catalysts. For Ni/ $\gamma$ -Al<sub>2</sub>O<sub>3</sub> and Ni/SiO<sub>2</sub>, the obvious CO<sub>2</sub> desorptions after 600 °C implied the existence of strong basic sites besides the weak and/or medium basic ones. As Ni was supported on ZnO, the weak, medium and strong basic sites co-existed but the amount of these sites was remarkably lowered than the other three catalysts. When La<sub>2</sub>O<sub>3</sub> was introduced, the weak and medium basic sites for Ni/La<sub>2</sub>O<sub>3</sub>/ZrO<sub>2</sub> and Ni/La<sub>2</sub>O<sub>3</sub>/ $\gamma$ -Al<sub>2</sub>O<sub>3</sub> were signifi-

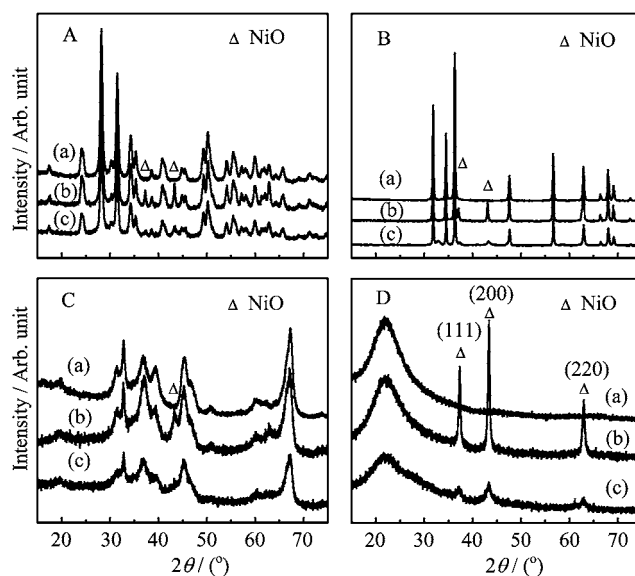


FIG. 1 The XRD patterns of Ni based catalysts with and without La<sub>2</sub>O<sub>3</sub>. A: (a) ZrO<sub>2</sub>, (b) 10%Ni/ZrO<sub>2</sub>, and (c) 10%Ni/10%La<sub>2</sub>O<sub>3</sub>/ZrO<sub>2</sub>. B: (a) ZnO, (b) 10%Ni/ZnO, and (c) 10%Ni/10%La<sub>2</sub>O<sub>3</sub>/ZnO. C: (a)  $\gamma$ -Al<sub>2</sub>O<sub>3</sub>, (b) 10%Ni/ $\gamma$ -Al<sub>2</sub>O<sub>3</sub>, and (c) 10%Ni/10%La<sub>2</sub>O<sub>3</sub>/ $\gamma$ -Al<sub>2</sub>O<sub>3</sub>. D: (a) SiO<sub>2</sub>, (b) 10%Ni/SiO<sub>2</sub>, and (c) 10%Ni/10%La<sub>2</sub>O<sub>3</sub>/SiO<sub>2</sub>.

cantly increased while with the strong basic sites reduced for the latter catalyst. However, a slightly increased basic sites were obtained for La<sub>2</sub>O<sub>3</sub> introducing to Ni/ZnO and Ni/SiO<sub>2</sub>. For comparison, the bulky La<sub>2</sub>O<sub>3</sub> showed three distinct CO<sub>2</sub> desorption peaks at 150, 350, and 500 °C (Fig.S2 in supplementary material), demonstrating the weak, medium and strong basic sites were concurrently presented with the strong one as the majority. Obviously, the basicities of the Ni-

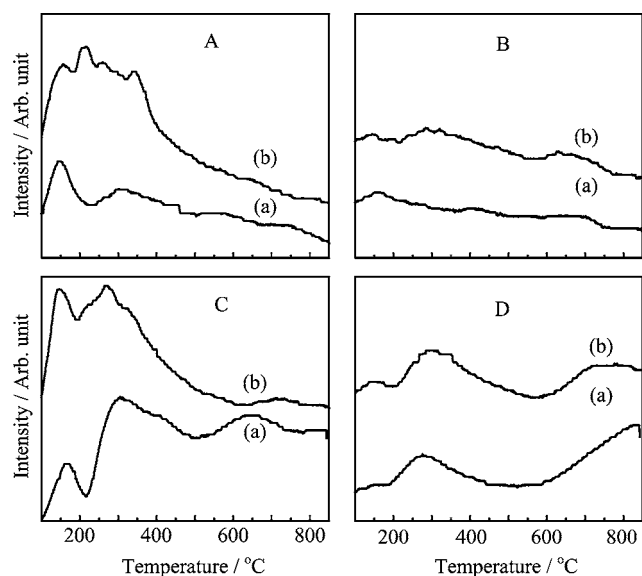


FIG. 2 The CO<sub>2</sub>-TPD curves of Ni based catalysts with and without La<sub>2</sub>O<sub>3</sub> additive.

A: (a) 10%Ni/ZrO<sub>2</sub>, (b) 10%Ni/10%La<sub>2</sub>O<sub>3</sub>/ZrO<sub>2</sub>.

B: (a) 10%Ni/ZnO, (b) 10%Ni/10%La<sub>2</sub>O<sub>3</sub>/ZnO.

C: (a) 10%Ni/γ-Al<sub>2</sub>O<sub>3</sub>, (b) 10%Ni/10%La<sub>2</sub>O<sub>3</sub>/γ-Al<sub>2</sub>O<sub>3</sub>.

D: (a) 10%Ni/SiO<sub>2</sub>, (b) 10%Ni/10%La<sub>2</sub>O<sub>3</sub>/SiO<sub>2</sub>.

based catalysts are strongly dependent on the interaction between support and La<sub>2</sub>O<sub>3</sub>, and La<sub>2</sub>O<sub>3</sub> supported on ZrO<sub>2</sub> [20, 21] and γ-Al<sub>2</sub>O<sub>3</sub> could largely retain the basic sites of the catalysts.

Considering the introduction of La<sub>2</sub>O<sub>3</sub> promoted the dispersities of Ni on catalyst surface, we further analyzed the H<sub>2</sub> reduction behavior of Ni based catalysts by H<sub>2</sub>-TPR technique (Fig.S3 in supplementary material). Without La<sub>2</sub>O<sub>3</sub>, the Ni/ZrO<sub>2</sub> and Ni/SiO<sub>2</sub> showed a single peak at about 420 °C, corresponding to the reduction of bulky NiO particles. As La<sub>2</sub>O<sub>3</sub> was added, apart from the H<sub>2</sub> reduction of bulky NiO particles, an additional peak was observed at 550 °C for Ni/La<sub>2</sub>O<sub>3</sub>/ZrO<sub>2</sub> and at 650 °C for Ni/La<sub>2</sub>O<sub>3</sub>/SiO<sub>2</sub>, respectively, indicating the reduction of NiO directly contacted with La<sub>2</sub>O<sub>3</sub> [18]. This is well consistent with the results obtained by the XRD patterns. For Ni supporting on ZnO and γ-Al<sub>2</sub>O<sub>3</sub>, the addition of La<sub>2</sub>O<sub>3</sub> or not showed very similar H<sub>2</sub> reduction profiles, which was possibly due to the easy formation of spinel structure for NiO/γ-Al<sub>2</sub>O<sub>3</sub> and some aggregated species for Ni/ZnO even in the presence of La<sub>2</sub>O<sub>3</sub> [12, 22]. These strong interactions led to the reduction of partial Ni<sup>2+</sup> at temperatures higher than 600 °C.

## B. Sorbitol hydrogenolysis

Table II presented the results of sorbitol hydrogenolysis over Ni based catalysts with different supports and basic additives at 220 °C and 4 MPa of initial H<sub>2</sub> pres-

sure. In this processing, the main products of glycerol, 1,2-PG and EG, and the byproducts such as xylitol, erythritol, isosorbide, methanol, ethanol, *etc.* were detected by the current analysis (the data of byproducts were not shown here).

The results of entry 1 to 4 in Table II indicated that the Ni-based catalysts exhibited low product selectivity when no basic additives were introduced even the significant sorbitol conversions were obtained over Ni/γ-Al<sub>2</sub>O<sub>3</sub> and Ni/SiO<sub>2</sub>. Among these pristine catalysts, the highest glycols (the sum of EG and 1,2-PG) yield was 30% over Ni/SiO<sub>2</sub>, which is possibly due to the strong basic sites of the catalyst which promoted hydrogenolysis of sorbitol to get more target products.

As La<sub>2</sub>O<sub>3</sub> was introduced to ZnO, γ-Al<sub>2</sub>O<sub>3</sub> and SiO<sub>2</sub> followed by impregnating Ni, the sorbitol conversions were reduced to different levels compared to the corresponding pristine catalysts (entry 6–8, Table II). On the other hand, the significantly increased sorbitol conversion and glycols yield were observed over the Ni/La<sub>2</sub>O<sub>3</sub>/ZrO<sub>2</sub> catalyst (entry 6, Table II). This indicates that the enhanced basicity on the catalyst can efficiently promote C–C bond cleavage to produce the glycerol and glycols, combined with the result of CO<sub>2</sub>-TPD result (Fig.2A). On the basis of Ni/ZrO<sub>2</sub>, we further compared the influence of basic La<sub>2</sub>O<sub>3</sub>, CeO<sub>2</sub>, MgO and CaO additives in the same process. The results of entry 5 and 9–11 in Table II indicated that both the sorbitol conversion and products selectivity increased when compared to the pristine catalyst without basic additive. Among these catalysts, La<sub>2</sub>O<sub>3</sub> and MgO exhibited the promising promotion effect because the higher sorbitol conversions and glycols yield could be gained.

Taking into account that La<sub>2</sub>O<sub>3</sub> showed the significantly enhanced effect, we investigated the influence of La<sub>2</sub>O<sub>3</sub> content on sorbitol hydrogenolysis with Ni/La<sub>2</sub>O<sub>3</sub>/ZrO<sub>2</sub> catalyst and the experimental results are listed in Table II (entry 12–16). With the La<sub>2</sub>O<sub>3</sub> content increasing from 2% to 40%, the sorbitol conversion and glycols yield presented the typical volcano tendency with the maximal activity of 97% at 5% of La<sub>2</sub>O<sub>3</sub> and 47% of yield at 10% of La<sub>2</sub>O<sub>3</sub>, respectively. Regarding the products, the glycerol selectivity showed the similar volcano to those obtained in the conversion, while EG and 1,2-PG remarkably increased with increasing La<sub>2</sub>O<sub>3</sub> from 2% to 5% and then changed a little as the amount of La<sub>2</sub>O<sub>3</sub> was more than 5%. Obviously, 10% of La<sub>2</sub>O<sub>3</sub> promoter presented as the optimal value based on its activity and target products yield in sorbitol hydrogenolysis.

Because the 10%Ni/10%La<sub>2</sub>O<sub>3</sub>/ZrO<sub>2</sub> catalyst showed the highest glycols yield, we further investigated the influence of reaction temperature and time in sorbitol hydrogenolysis and the results are revealed in Fig.3. The sorbitol conversion increased with increasing the reaction temperature and can be completely converted at 240 °C. Meanwhile, glycerol raised slightly and obtained the highest selectivity of

TABLE II Sorbitol hydrogenolysis over different Ni based catalysts<sup>a</sup>.

Entry	Catalyst	Conversion/%	Products selectivity <sup>b</sup> /%			Total glycols selectivity/%
			Glycerol	EG	1,2-PG	
1	10%Ni/ZrO <sub>2</sub>	32.0	19.5	5.6	6.8	12.4
2	10%Ni/ZnO	33.1	6.9	7.4	21.2	28.6
3	10%Ni/ $\gamma$ -Al <sub>2</sub> O <sub>3</sub>	58.5	20.2	4.5	4.2	8.7
4	10%Ni/SiO <sub>2</sub>	73.4	7.9	14.0	27.1	41.1
5	10%Ni/10%La <sub>2</sub> O <sub>3</sub> /ZrO <sub>2</sub>	71.3	26.7	15.5	25.4	40.9
6	10%Ni/10%La <sub>2</sub> O <sub>3</sub> /ZnO	14.6	2.8	15.5	24.0	39.5
7	10%Ni/10%La <sub>2</sub> O <sub>3</sub> / $\gamma$ -Al <sub>2</sub> O <sub>3</sub>	46.7	22.8	14.7	22.3	37.0
8	10%Ni/10%La <sub>2</sub> O <sub>3</sub> /SiO <sub>2</sub>	52.4	29.9	8.7	14.3	23.0
9	10%Ni/10%CeO <sub>2</sub> /ZrO <sub>2</sub>	47.1	27.6	14.6	25.3	39.9
10	10%Ni/10%MgO/ZrO <sub>2</sub>	67.8	23.2	14.3	34.5	48.8
11	10%Ni/10%CaO/ZrO <sub>2</sub>	39.4	19.4	14.9	28.1	43.0
12	10%Ni/2%La <sub>2</sub> O <sub>3</sub> /ZrO <sub>2</sub>	61.3	20.1	6.8	12.1	18.9
13	10%Ni/5%La <sub>2</sub> O <sub>3</sub> /ZrO <sub>2</sub>	97.2	29.6	16.1	28.4	44.5
14	10%Ni/10%La <sub>2</sub> O <sub>3</sub> /ZrO <sub>2</sub>	96.5	23.3	17.5	30.7	48.2
15	10%Ni/20%La <sub>2</sub> O <sub>3</sub> /ZrO <sub>2</sub>	89.8	21.9	16.6	28.4	45.0
16	10%Ni/40%La <sub>2</sub> O <sub>3</sub> /ZrO <sub>2</sub>	86.6	21.6	16.4	28.8	45.2

<sup>a</sup> Reaction conditions: sorbitol of 20 mL (100 mg/mL sorbitol aqueous solution), initial H<sub>2</sub> pressure: 4 MPa, reaction temperature: 220 °C, catalysts dosage: 0.4 g. Reaction time: 3 h for entry 1–11, 4 h for entry 12–16.

<sup>b</sup> Only the target products are considered and other byproducts including xylitol, erythritol, isosorbide, methanol, ethanol aren't shown here.

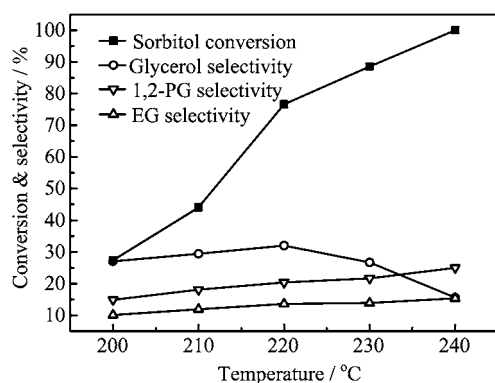


FIG. 3 Effect of reaction temperature on sorbitol hydrogenolysis over 10%Ni/10%La<sub>2</sub>O<sub>3</sub>/ZrO<sub>2</sub>. Reaction condition: 4 MPa of initial H<sub>2</sub> pressure, 220 °C and 2 h.

33% until the temperature rose to 220 °C followed by decreasing to 15% as the temperature further increased to 240 °C. On the other hand, higher temperature is benefited for the formation of EG and 1,2-PG but with much slower increase rate than the conversion. This indicated that the glycerol is the intermediate and could be further converted to 1,2-PG by C–O bond cleavage at increased temperatures [23]. The higher temperatures enhanced sorbitol conversion but also accelerated further degradation of target products such as EG and 1,2-PG and mainly obtained the byproducts propanol, ethanol, methanol and CH<sub>4</sub>, which

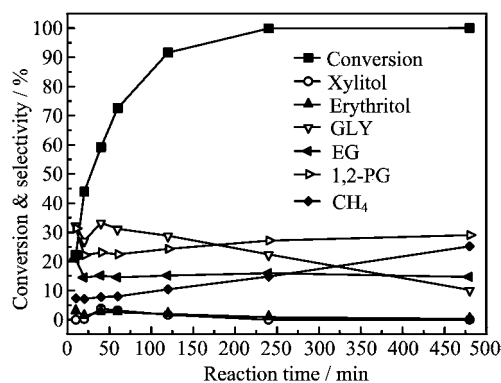


FIG. 4 The influence of reaction time for sorbitol hydrogenolysis. Reaction condition: 4 MPa of initial H<sub>2</sub> pressure, 220 °C.

implies the typical consecutive reaction for sorbitol hydrogenolysis (Fig.S4 in supplementary material).

The influence of reaction time showed the similar trend to reaction temperature dependent on sorbitol conversion and products distribution (Fig.4). With hydrogenolysis proceeding, sorbitol conversion increased rapidly and completely converted at 4 h. Compared with 1,2-PG, EG selectivity presented slower increasing rate and changed a little after 4 h. At 8 h, the total selectivity of EG and 1,2-PG reached the maximum 48% with 100% of sorbitol conversion, which indicated that the prepared catalyst performed high activity and diols

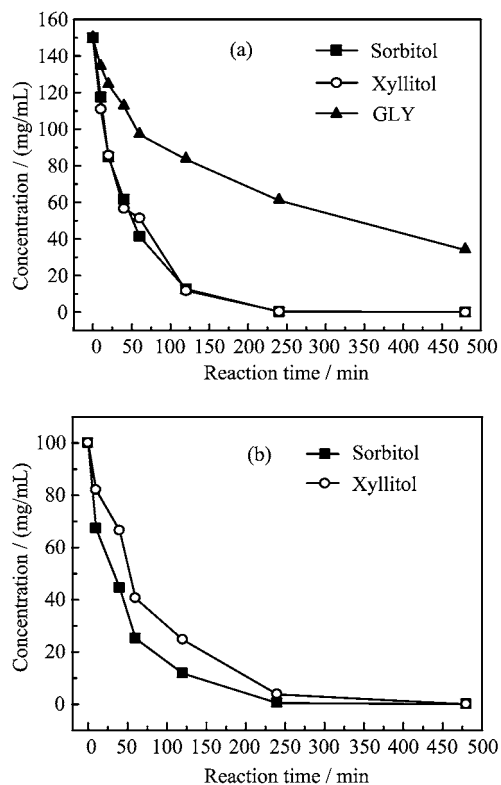


FIG. 5 (a) The concentration-time curves of polyols hydrogenolysis (sorbitol, xyllitol, and glycerol). Reaction condition: 4 MPa of initial  $H_2$  pressure, 220 °C. (b) Hydrogenolysis of mixture.

yield in this process. To discuss the pathway of sorbitol hydrogenolysis, we also analyzed some byproducts, such as xyllitol, erythritol, gas products and so on. The curves indicated that the selectivity of  $CH_4$  increased gradually during sorbitol hydrogenolysis, however, the selectivity of xyllitol and erythritol still remained low always. It seemed that the Ni-based catalyst tended to promote the C3–C4 bond cleavage of sorbitol.

We also studied the kinetic processes of different polyols under the same condition to find out how sorbitol and its intermediates influence the distribution of final products (Fig.4, Fig.5, and Fig.6). Firstly, the activity of hydrogenolysis was related to the hydroxyl number of reactant, and sorbitol had the highest activity. Figure 5 shows the concentration-time curves of polyols. The curves indicated that sorbitol had higher activity and there might be some competitive mechanism among different polyols. The polyols with more hydroxyl number would perform better activity which indicated the multi-points adsorption of polyols on catalyst. Secondly, glycerol hydrogenolysis [23] showed low activity and simple products distribution, which would be useful to analyze hydrogenolysis mechanism. The average selectivity of C–O cleavage product (1,2-PG) and C–C cleavage products ( $CH_4$  and EG) were 72% and 24%, respectively. EG had almost the same se-

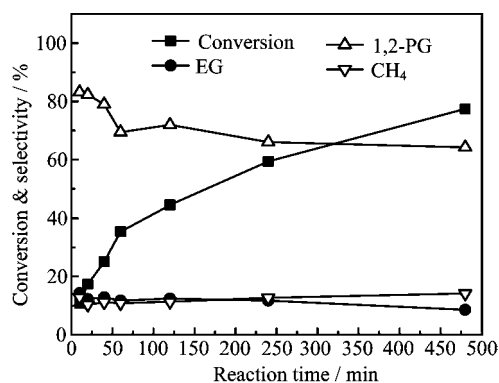


FIG. 6 The influence of reaction time for glycerol hydrogenolysis. Reaction condition: 4 MPa of initial  $H_2$  pressure, 220 °C.

lectivity as  $CH_4$ , which indicated that  $CH_4$ :EG (molar ratio) was about 2:1. Based on the above analysis, glycerol hydrogenolysis underwent both C–C bonds cleavage simultaneously, which revealed that the complicity of polyols hydrogenolysis.

Sorbitol hydrogenolysis was a complex process and its products distribution was final results of kinetic balance of polyols hydrogenolysis. Xyllitol and erythritol were intermediates which can be adsorbed above catalysts preferentially and then hydrogenolyzed quickly, and that resulted in no accumulation of xyllitol and erythritol because of competitive mechanism of polyols hydrogenolysis.

#### IV. CONCLUSION

We prepared bi-functional Ni based catalysts with different supports and basic additives for sorbitol hydrogenolysis by sequential impregnation method. Introduction of basic additives enhanced basicities of Ni based catalyst and promoted dispersities of Ni particles by strong interactions of  $Ni^{2+}$  and basic additives. By screening the catalysts, 10%Ni/10% $La_2O_3$ / $ZrO_2$  showed superior catalytic performance for sorbitol hydrogenolysis. The synergistic effect of  $La_2O_3$  and Ni improved sorbitol hydrogenolysis to produce glycerol, EG and 1,2-PG with the highest glycols (EG and 1,2-PG) yield of 48% obtained at optimal reaction condition. The kinetics study of polyols (sorbitol, xyllitol, and glycerol) hydrogenolysis showed that polyols with more hydroxyl number have higher activity and products distribution was final results of kinetic balance, which could give us some inspiration about how to change the products selectivity.

**Supplementary material:** Some characterization results were listed in supplementary information, such as XRD patterns of  $ZrO_2$  and different base modified catalysts, the  $CO_2$ -TPD curve of  $La_2O_3$ , the  $H_2$ -TPR profiles of the Ni based catalysts with and without

La<sub>2</sub>O<sub>3</sub> additive, HPLC patterns of sorbitol hydrogenolysis.

## V. ACKNOWLEDGMENTS

This work was supported by the National Natural Science Foundation of China (No.51376185 and No.51106108), the National Basic Research Program of China (No.2012CB215304), the National High Technology Research and Development Program of China (No.2012AA101806), and the Natural Science Foundation of Guangdong Province (No.S2013010011612).

- [1] A. M. Ruppert, K. Weinberg, and R. Palkovits, *Angew. Chem.* **51**, 2564 (2012).
- [2] Y. Nakagawa and K. Tomishige, *Catal. Surveys. Asia* **15**, 111 (2011).
- [3] J. Zhang, S. B. Wu, and Y. Liu, *Ind. Eng. Chem. Res.* **52**, 11799 (2013).
- [4] K. Sohounloue, *React. Kinet. Catal. Lett.* **22**, 391 (1983).
- [5] Y. Yoo and D. K. Kim, *Poly. J.* **30**, 538 (1998).
- [6] G. W. Huber and C. Avelino, *Chem. Rev.* **106**, 55 (2006).
- [7] K. Wang and T. D. Furney, *Ind. Eng. Chem. Res.* **34**, 3766 (1995).
- [8] K. Wang, M. C. Hawley, and T. D. Furney, *Chem. Eng. Sci.* **58**, 4271 (2003).
- [9] M. Banu, S. Sivasanker, T. M. Sankaranarayanan, and P. Venuvanalingam, *Catal. Comm.* **12**, 673 (2011).
- [10] X. G. Chen, X. C. Wang, S. X. Yao, and X. D. Mu, *Catal. Comm.* **39**, 86 (2013).
- [11] Z. W. Huang, J. Chen, Y. Q. Jia, H. L. Liu, C. G. Xia, and H. C. Liu, *Appl. Catal. B* **147**, 377 (2014).
- [12] L. M. Ye, X. P. Duan, H. Q. Lin, and Y. Z. Yuan, *Catal. Today* **183**, 65 (2012).
- [13] H. L. Liu, Z. W. Huang, J. Chen, Y. Q. Jia, C. G. Xia, and H. C. Liu, *ChemCatChem* **6**, 2918 (2014).
- [14] J. H. Zhou, L. Zhao, Z. J. Sui, and X. G. Zhou, *Chem. Eng. Sci.* **65**, 30 (2010).
- [15] N. Li and G. W. Huber, *J. Catal.* **270**, 48 (2010).
- [16] L. Zhao, J. H. Zhou, H. Chen, M. G. Zhang, Z. J. Sui, and X. G. Zhou, *Korean J. Chem. Eng.* **27**, 1412 (2010).
- [17] M. Banu, P. Venuvanalingam, R. Shanmugam, B. Viswanathan, and S. Sivasanker, *Top. Catal.* **55**, 897 (2012).
- [18] J. Gao, Z. Y. Hou, J. Z. Guo, Y. H. Zhu, and X. M. Zheng, *Catal. Today* **131**, 278 (2008).
- [19] F. Wang, R. J. Shi, Z. Q. Liu, P. J. Shang, X. Y. Pang, S. Shen, Z. H. Feng, C. Li, and W. J. Shen, *ACS Catal.* **3**, 890 (2013).
- [20] H. Sun, Y. Q. Ding, J. Z. Duan, Q. J. Zhang, Z. Y. Wang, H. Lou, and X. M. Zheng, *Bioresour. Technol.* **101**, 953 (2010).
- [21] M. B. I. Chowdhury, M. M. Hossain, and P. A. Charpentier, *Appl. Catal. A* **405**, 84 (2011).
- [22] J. Y. Hu, X. Y. Liu, B. Wang, Y. Pei, M. H. Qiao, and K. N. Fan, *Chin. J. Catal.* **33**, 1266 (2012).
- [23] M. A. Dasari, P. P. Kiatsimkul, W. R. Sutterlin, and G. J. Suppes, *Appl. Catal. A* **281**, 225 (2005).